HHS Public Access

Author manuscript

Nat Med. Author manuscript; available in PMC 2016 July 25.

Published in final edited form as:

Nat Med. 2016 March ; 22(3): 312–318. doi:10.1038/nm.4031.

Human ‘brite / beige’ adipocytes develop from capillary networks and their implantation improves metabolic homeostasis in mice

So Yun Min[1,2], **Jamie Kady**[1,3], **Minwoo Nam**[2,4], **Raziel Rojas-Rodriguez**[1,2], **Aaron Berkenwald**[5], **Jong Hun Kim**[1], **Hye-Lim Noh**[1], **Jason K. Kim**[1], **Marcus P. Cooper**[4], **Timothy Fitzgibbons**[4], **Michael A. Brehm**[1,3], and **Silvia Corvera**[1,6]

[1]Program in Molecular Medicine, University of Massachusetts Medical School, Worcester, MA

[2]Graduate School of Biomedical Sciences, University of Massachusetts Medical School, Worcester, MA

[3]Diabetes Center of Excellence, University of Massachusetts Medical School, Worcester, MA

[4]Cardiovascular Center of Excellence, University of Massachusetts Medical School, Worcester, MA

[5]Clinical Translational Research Pathway, University of Massachusetts Medical School, Worcester, MA

Abstract

The uncoupling protein 1 (UCP1) is highly expressed in brown adipose tissue, where it generates heat by uncoupling electron transport from ATP production. UCP1 is also found outside classical brown adipose tissue depots[1–4], in adipocytes termed ‘brite’ (brown-in-white) or ‘beige’. In humans, the presence of ‘brite/beige’ adipocytes correlates with a lean, metabolically healthy phenotype[5–8], but whether a causal relationship exists is not clear. Here we report that human ‘brite/beige’ adipocyte progenitors proliferate in response to pro-angiogenic factors, in association with expanding capillary networks. Adipocytes formed from these progenitors transform from being UCP1-negative to UCP1-positive in response to adenylate cyclase activation, a defining feature of the ‘beige/brite’ phenotype, and display uncoupled respiration. When implanted into normal or high fat diet-fed, glucose intolerant NOD-*scid IL2rg*^{null} mice, activated ‘brite/beige’ adipocytes enhance systemic glucose tolerance. These adipocytes express neuroendocrine and secreted factors, including the pro-protein convertase *PCSK1*, which is strongly associated with human obesity. Thus, pro-angiogenic conditions drive proliferation of human ‘beige/brite’

[6]**Corresponding Author**. Silvia Corvera M.D., ; Email: silvia.corvera@umassmed.edu

Accession codes

Data files for Affymetrix HTA-2 arrays can be found at GEO Accession number GSE73385

Author contributions

SYM, SC, MAB and MPC designed the experiments; SYM and RRR obtained adipose tissue, generated cells, and performed experiments on cells; JK and SYM performed experiments on mice; AB, MN, TF and MPC obtained and analyzed perivascular adipose tissue samples; JHK, HLN and JKK performed and analyzed metabolic phenotyping experiments. SYM and SC wrote the manuscript. All authors contributed to editing the manuscript. SC managed the project.

Competing financial interests.

The authors disclose no competing financial interests.

adipocyte progenitors, and activated ‘beige/brite’ adipocytes can affect systemic glucose homeostasis, potentially through a neuroendocrine mechanism.

Keywords

human adipocyte; glucose; cytokine; adipokine; thermogenic adipose tissue; implant; capillary; progenitors; adrenergic

---

During human embryonic development adipocytes first appear from emergent vascular networks[9], and lineage-tracing studies have demonstrated that adipocyte progenitors reside within the walls of adult mouse adipose tissue capillaries[10–13]. These findings suggest that proliferation of adipocyte and vascular progenitors may be interdependent. To determine whether human adipocyte progenitors proliferate in conjunction with adipose tissue capillaries we used an *in vitro* system in which microvessels develop from adipose tissue fragments *in vitro* (Online methods). Explants from human subcutaneous adipose tissue from individuals undergoing panniculectomy surgery (Supplementary Table 1) were embedded in Matrigel and cultured in DMEM (Dulbecco’s Modified Eagle’s Medium) + 10% FBS (Fetal Bovine Serum), or in EGM2-MV (Endothelial Cell Growth Medium-Microvascular) in the absence or presence of pro-angiogenic growth factors VEGF (vascular endothelial growth factor), hFGF-B (human fibroblast growth factor B), hEGF (human epidermal growth factor), R^3-IGF-1 (long R3 insulin-like growth factor 1) (Fig. 1a), and imaged after 10 days in culture. Capillary growth was negligible in explants cultured in either DMEM of EGM-2 MV in the absence of growth factors, but clearly measurable in DMEM or EGM-2 MV in their presence (Fig. 1b). Maximal growth was seen in EGM2-MV, consistent with the optimized pro-angiogenic properties of this medium. Over time cells at the tips of the sprouts projected thin filopodia into the gel, divided, and aligned to form thicker branches (Fig. 1c), which previously have been seen to include endothelial and non-endothelial cells[14,15]. To determine whether any of these cells correspond to adipocyte progenitors, we exposed cultures to adipogenic conditions. Because activation of PPARγ (peroxisome-proliferator activated receptor gamma) by ligands such as thiazolidenediones can induce lipid accumulation in cells independently of adipogenic conversion[16], we used a minimal adipogenic cocktail of 3-isobutyl-1-methylxanthine, dexamethasone and insulin (MDI). After approximately 6 days, we observed a loss of continuity between cells forming the capillary structure, and lipid droplets in cells within the capillaries (Fig. 1c). These morphological changes were accompanied by induction of classical adipocyte markers (Fig. 1d). These results were reproduced in explants from all panniculectomy samples studied (Supplementary Table 1), albeit the magnitude of the induction of individual markers varied. Thus, proliferation of human adipocyte progenitors occurred in conjunction with capillary growth, and is critically dependent on pro-angiogenic growth factors.

To determine whether proliferation and/or differentiation of adipocyte progenitors required intercellular interactions within the capillary, or on interactions with Matrigel components, we generated single-cell suspensions from the microvessels, passaged them once on standard tissue culture dishes and subjected them to differentiation. Numerous cells differentiated into adipocytes, identifiable by lipid droplets that increased in size and coalesced over time (Fig

1e, arrows), and by the induction of adipocyte genes (Fig. 1f). Results shown were similar in capillary network cells from all explants studied, albeit the magnitude of the induction of individual genes varied. To determine whether single adipocyte progenitors are capable of autonomous growth and differentiation, live single cells were individually sorted into wells of 384 well plates. As expected from cells of non-hematopoietic lineage, these cells were $CD45^{-}$ (Supplementary Fig. 1). Surviving colonies (approximately 10% of seeded wells) could be further passaged into 96 well multiwells; of these, approximately 75% underwent adipogenic differentiation, as determined morphologically by lipid droplet accumulation (Fig. 1g), and functionally by secretion of adiponectin into the culture medium (Fig. 1h). Thus, human adipocyte progenitors isolated from capillary networks can be clonally expanded and can undergo differentiation in a cell autonomous manner.

To determine whether cells generated from capillary networks include 'brite/beige' adipocytes, we stimulated cultures acutely and chronically with the adenylate cyclase activator forskolin, and analyzed thermogenic gene expression by RT-PCR (Fig. 2a). *UCP1* mRNA was almost undetectable before and after adipogenic differentiation, but was induced rapidly in response to forskolin, and remained elevated in response to chronic exposure to the drug, as were canonical brown fat cell genes *CIDEA* (cell death inducing DFFA-like effector a) and *DIO2* (deiodinase 2) (Fig. 2a). We also detected genes previously identified in mouse adipocyte progenitors, including *CD29* (integrin beta 1), *CD24* (cluster of differentiation 24), *PDGFRA* (platelet-derived growth factor receptor alpha) and *ZNF423* (zinc finger protein 423), or enriched in 'brite/beige' adipocytes and human and mouse adipose tissue[17] (Supplementary Fig. 2). To determine whether cells responded to physiological stimuli that cause "browning" *in vivo*, we compared the responses of non-differentiated and differentiated cells to forskolin and isoproterenol (Fig. 2b). No induction was seen in non-differentiated cells, but differentiated adipocytes responded to both stimuli (Fig. 2b). Notably, the human-selective β3 adrenergic agonist Mirabegron, which activates human supraclavicular fat[18], was more potent than the murine-selective β3 agonist CL316,243 in inducing *UCP1* expression in differentiated cells (Fig. 2b), consistent with the presence of functional β3 adrenergic receptors in these human adipocytes. The increase in *UCP1* mRNA levels translated into an increase in protein as UCP1 was detected by immunofluorescence in most adipocytes, and progressively increased in abundance upon chronic exposure to forskolin (Fig. 2c). Mitochondria containing UCP1 were rounded, dense and abundant (Fig. 2d), a feature reminiscent of brown adipose tissue mitochondria[19]. In contrast, interspersed cells containing no detectable UCP1 contained the linear, sparse mitochondria (Fig. 2d).

The UCP1 expressed in these cells was functional, as cells treated chronically with forskolin displayed enhanced basal and uncoupled oxygen consumption (Fig. 2e), and mitochondrial parameters following addition of specific inhibitors (Fig. 2f) revealed decreased ATP-linked oxygen consumption and enhanced proton leak. The enhanced proton leak was at least in part attributable to the presence of UCP1, as respiratory rate was inhibited in response to 1 mM GDP in digitonin-permeabilized cells (Fig. 2g). Other changes consistent with known properties of thermogenic adipocytes were also seen, including the remodeling of large lipid droplets into numerous small lipid droplets (Fig. 2h)[20,21], accompanied by a large increase in expression of *PLIN1* (perilipin-1) (Fig 2i), consistent with an increase in droplet surface.

Increased expression of *FABP4* (fatty acid binding protein 4) and *SLC2A4* (Glut 4), involved in uptake of lipids and glucose, and changes in expression of *LEP* (leptin) (decreased) and *ADIPOQ* (adiponectin) (increased) were observed (Fig 2i), a pattern consistent with circulating concentrations of these adipokines in mice treated with 'pro-browning' β3 adrenergic agonists[22]. Thus, adipocytes derived from human capillary networks possess the cardinal biochemical and physiological characteristics of 'brite/beige' cells.

To determine the similarity of 'brite/beige' adipocytes generated from capillary networks to human thermogenic fat we obtained peri-carotid adipose tissue from four individuals undergoing elective carotid endarterectomy (Supplementary Table 1). Relative to the expression of *ADIPOQ*, significant variability in *UCP1* and *DIO2* levels amongst samples of peri-carotid fat was observed (Fig. 3a), but higher values were comparable to those seen in 'brite/beige' adipocytes from capillary networks. Thus, these adipocytes resemble thermogenic adipose tissue in humans. We next asked whether human 'brite/beige' cells could be functional *in vivo*. Cells were grown, differentiated, and stimulated with forskolin as described in Online Methods. We routinely obtained cultures with unilocular and multilocular adipocytes, collected them by trypsinization, resuspended them in Matrigel and implanted them into the dorsal region of NOD-*scid IL2rg*^{null} (NSG) mice (Fig 3b). After up to 11 weeks following implantation we observed only solidified remains of the gel in the dorsal region under the skin of mice receiving only Matrigel (Fig. 3b). In contrast, we observed well-delineated vascularized adipose tissue structures in mice implanted with cell suspensions (Fig. 3b). These structures were clearly demarcated from surrounding tissue and contained large patches of adipocytes and vasculature (Fig. 3c). Human adipocytes were viable and integrated into the mouse circulation, as we detected human adiponectin in serum from mice harboring implanted cells, but not in mice receiving Matrigel only (Fig. 3d). Remarkably, implanted adipocytes maintained the 'brite/beige' phenotype, as we detected human-specific *UCP1* and *PLIN1* expression in the adipose tissue structure at levels comparable to those found in cells prior to implantation (Fig. 3e), and we observed multilocular adipocytes in the excised structure (Supplementary Fig. 3).

We next asked whether human 'brite/beige' cells could affect glucose metabolism. Mice implanted with cells displayed lower fasting glucose (Fig. 3f) and a more rapid glucose disposal rate (Fig. 3g) compared to those receiving Matrigel only. NSG mice have been reported to be highly resistant to high fat diet-induced obesity[23]. Because susceptibility to high-fat diet (HFD) induced obesity and glucose intolerance are enhanced by thermoneutrality[24], we subjected a cohort of NSG mice to a HFD at 30°C. Within 2 weeks mice displayed significant glucose intolerance (Fig. 3h). At 2 weeks of HFD feeding, mice were randomized to receive Matrigel or 'brite/beige' adipocytes as above. Seven weeks following implantation, glucose tolerance was higher (Fig. 3i) and liver steatosis was lower (Fig. 3j) in mice receiving cells compared to those receiving only Matrigel. Thus, 'brite/beige' adipocytes derived from human capillary networks can enhance glucose metabolism in mice under normal conditions and in the context of impaired glucose tolerance.

While to our knowledge this is the first description of transplanted human adipocytes improving systemic glucose homeostasis, it has been reported that mouse subcutaneous

adipose tissue can improve glucose homeostasis in HFD-fed mice[25]. To determine whether the improvement in glucose tolerance seen in mice implanted with capillary-derived human adipocytes was indeed attributable to their 'brite/beige' characteristics, we compared the effects of non-activated versus forskolin-activated adipocytes. We used *in vivo* hyperinsulinemic-euglycemic clamps to measure whole body glucose turnover, which was normalized to circulating human adiponectin to adequately control for the quantity and functional integration of implanted human cells. Mice implanted with forskolin-activated cells displayed higher glucose turnover compared to those implanted with non-stimulated cells (Fig. 4a), demonstrating that the 'brite/beige' phenotype directly contributed to improved glucose metabolism. Indeed this value is likely to be underestimated, as adiponectin expression is higher in activated 'brite/beige' adipocytes (Fig. 2i). We noted a strong correlation between serum human adiponectin and whole body glucose turnover when the entire cohort of mice with non-activated and activated cells were analyzed (Fig. 4b), suggesting that non-activated cells were also capable of affecting glucose turnover, or that the cells became activated following transplantation. RT-PCR analysis of the implanted structures revealed detectable *UCP1* expression in tissue formed from non-activated cells, albeit at lower levels than that seen in tissue formed from forskolin-activated cells (Fig. 4c). These results support the conclusion that cells derived from human capillary networks give rise to 'brite/beige' adipocytes, which can be activated *in vitro* and *in vivo*, and can positively affect glucose homeostasis.

To determine whether the enhanced glucose tolerance seen in mice implanted with 'brite/beige' adipocytes was related to the thermogenic properties of these cells, body temperature was measured using subcutaneously implanted Thermochron iButton temperature loggers, which have a resolution of 0.025°C, set to record at 30 min intervals. Mice bred at room temperature harboring 'brite/beige' adipocytes did not differ significantly from Matrigel controls in their basal body temperature, or in their response to cold exposure (Fig. 4d). It remains possible that local thermogenic effects, undetectable by whole body temperature measurements, contribute to improved glucose metabolism. Alternatively, implanted cells might contribute to glucose tolerance independently of thermogenesis. To determine whether glucose uptake into implanted cells contribute to glucose turnover, we measured 2-[^{14}C] deoxyglucose uptake into tissues during hyperinsulinemic-euglycemic clamps. On a per gram of tissue basis, the rate of glucose uptake by implanted cell structures was significantly higher compared to epididymal white fat, but lower than interscapular brown fat in the same animal (Fig. 4e). Because the density of cells in the implant is lower than in tissue due to dilution with Matrigel, these values may represent an underestimate of glucose consumption by human cells. Thus, improved glucose tolerance may be in part attributable to glucose consumption by implanted cells. However, whole body glucose turnover was not directly correlated with the amount of glucose uptake by the implanted cells (Fig. 4f), suggesting that additional effects on peripheral tissues underlie enhanced glucose turnover. Indeed, improved metabolism attributable to brown adipose tissue effects on liver has been reported[26].

To explore the possibility that the metabolic benefits of human 'brite/beige' adipocytes could be due to secreted factors, we conducted global gene expression analysis of adipocytes before and after 7 days of forskolin stimulation (Fig. 4g). Unexpectedly, amongst the most

significantly induced genes were the proprotein-convertase subtilisin/kexin type-1 (*PCSK1*), its substrate proenkephalin (*PENK*), and interleukin 33 (*IL-33*), which were also detected in human peri-carotid fat (Fig. 4h). Mutations and polymorphisms in *PCSK1* are strongly associated with human obesity[27,28], although the underlying mechanisms are unclear. Cleavage of PENK by PCSK1 produces enkephalins, which are made in peripheral tissues in addition to the brain[29]. IL-33 has been shown to decrease adiposity, mitigate atherosclerosis and be necessary for normal glucose homeostasis in mouse models[30,31]. Interestingly, enkephalins and IL-33 have been shown to induce adipose tissue browning[31]; thus, production of these factors by implanted 'brite/beige' cells could explain the sustained expression of *UCP1* seen weeks following implantation (Fig. 3e). While we were not able to detect IL-33 in the circulation of transplanted mice, immunostaining revealed punctate structures containing IL-33 within activated adipocytes (Supplementary Fig. 4). Further studies will be required to determine possible autocrine effects of IL-33 on the induction or maintenance of the 'brite/beige' adipocyte phenotype *in vivo*.

In summary, our data reveal that human adipocyte progenitor cells proliferate in response to pro-angiogenic stimuli in conjunction with adipose tissue angiogenesis. These cells display the cardinal feature of 'brite/beige' adipocytes, which is the near absence of thermogenic genes under basal condition, but their strong induction in response to adrenergic stimulation. To our knowledge, these findings are the first to enable the growth and differentiation of human 'brite/beige' cells, and the assessment of their effects of systemic glucose homeostasis. These cells differ from human brown adipocyte cell lines established through immortalization of human precursors[32,33] or differentiation of human pluripotent stem cells[34] in their highly inducible expression of a thermogenic phenotype, in the development of uncoupled respiration, and in their capacity to affect metabolism upon transplantation *in vivo*.

Our finding of a functional relationship between angiogenesis and 'brite/beige' adipocyte development converges with existing studies where overexpression of the pro-angiogenic factor VEGF in mouse adipose tissue results in extensive browning[35,36]. In addition, perivascular adipose tissue surrounding major blood vessels displays thermogenic characteristics[37,38], and its loss results in cold intolerance, endothelial dysfunction and susceptibility to atherosclerosis[37]. The finding that human 'brite/beige' adipocytes enhance glucose homeostasis provides a clear rationale for their potential therapeutic use. Moreover, the expression of neuroendocrine and secreted factors by activated cells suggests that secreted products identified in these studies could also contribute to metabolic effects. Future studies to systematically assess the mechanisms by which human 'brite/beige' cells develop and affect glucose homeostasis will be greatly facilitated by the ability to generate these cells from human adipose tissue by the methods described herein.

Online Methods

General Methodology

No samples, mice or data points were excluded from the reported analyses. Samples were not randomized to experimental groups except where indicated. Analyses were not performed in a blinded fashion except where noted below.

Materials

Matrigel from BD biosciences (356231); EGM-2 MV from Lonza; Anti-human UCP1 antibody from Abcam (ab10983); anti Heat Shock Protein 70 from ThermoFisher Scientific (MA3-028); anti human IL33 from ThermoFisher Scientific (PA5-20397); Adiponectin human-specific ELISA kits from Invitrogen (KHP0041); Forskolin and Isoproterenol hydrochloride from Sigma (F3917 and I6504, respectively). iButtons were purchased from Embedded Data Systems, DS1922L-F5#)

Adipose Tissue

Subcutaneous adipose tissue was obtained from panniculectomies, and peri-carotid adipose tissue from elective vascular surgeries with no a-priori selection of individual donors. All specimens were collected after informed consent in accordance with procedures approved by the University of Massachusetts Institutional Review Board. The characteristics of patients from which tissues were used for indicated experiments are described (Supplementary table 1).

Explants

Detailed methods for harvesting adipose tissue, culture of adipose tissue explants in Matrigel are published[39]. In brief, explants from human subcutaneous adipose tissue were cultured in EBM-2 media supplemented with endothelial growth factors (EGM-2 MV) (Lonza). In indicated experiments, Dulbecco's Modified Eagles Medium (Gibco) supplemented with 10% fetal bovine serum ((DMEM-FBS) was used, without or with supplementation with hFGF-B, hEGF, R3-IGF1 and VEGF at the concentrations used in EGM2-MV, as indicated. To induce adipogenesis we used a minimal adipogenic cocktail of DMEM +10% FBS, 0.5 mM 3-isobutyl-1-methylxanthine, 1μM dexamethasone, and 1μg/ml insulin (MDI) for 72h. The medium was then replaced with DMEM plus 10% FBS. Subsequently, 50% of the medium was replaced with fresh medium every other day. Adipocyte markers were measured by RT-PCR in RNA extracted from 3 explants per condition. Results shown in Figure 1 were reproduced in explants from all panniculectomy samples studied (Supplementary Table 1), albeit the magnitude of the induction of individual markers varied.

Cells

Detailed methods for harvesting adipose tissue, culture of adipose tissue explants in Matrigel, and harvesting of single cells from explant growth are published[39]. In brief, explants from human subcutaneous adipose tissue were cultured in EBM-2 media supplemented with endothelial growth factors (EGM-2 MV) (Lonza) for 14 days. Single cells suspensions from capillary growth (capillary network cells) were obtained using dispase[39], and plated on standard tissue culture plates. Growth and passaging of these cells was done using EGM-2 MV. Where indicated, adipogenic differentiation was induced by replacement of EGM-2 MV by DMEM +10% FBS, 0.5 mM 3-isobutyl-1-methylxanthine, 1μM dexamethasone, and 1μg/ml insulin (MDI). 72 hr later, the differentiation medium was replaced by DMEM-FBS, which was replaced every 48 hours until analysis. Adipocyte markers were measured by RT-PCR in RNA extracted from one well of a confluent 6 well multiwell dish of cells. To obtain clonal populations, single cells suspensions were obtained

from capillary network cell cultures using trypsin, stained with 7-amino-actinomycin D (7-AAD) for live/dead cell identification, and sorted into individual wells of 384 well multiwell dishes using a BSL3 BD FACSAria Cell Sorter (BD Biosciences). Clones were grown and expanded using EGM-2 MV. Viable clones were passaged onto 96 well multiwell dishes, differentiated as described above, and used for experiments described. Cells were not routinely tested for mycoplasma contamination. Adiponectin concentration in the culture medium was measured using a human-specific adiponectin ELISA from Invitrogen (KHP0041). For analysis of thermogenic gene expression, isoproterenol and forskolin were used at final concentrations of 10 and 50 μM, unless otherwise indicated in the figures.

In experiments to investigate the effects of 'brite/beige' adipocytes *in vivo*, cells from capillary networks were grown to confluence into 150 mm dishes, differentiated using MDI for 10 days, and browning induced for 7 days with forskolin. Cells were then were recovered from culture dishes by trypsin-collagenase digestion, suspended in Matrigel and injected (approximately 10^7 cells per mouse) into the dorsal region of male NOD-*scid IL2rg*^{null} (NSG) mice[40].

RT-PCR

Adipocyte markers were measured in RNA extracted from 3 explants per condition, or from one well of a confluent 6 well multiwell dish of cells. Probe sets used are shown in Supplementary Table 2.

Immunofluorescence

Cells were fixed in 4% formaldehyde, stained, mounted and imaged with a Zeiss Axiovert 100 inverted microscope and AxioCam HRm camera. Image processing and quantification was performed using ImageJ (FIJI) software, on a file containing all raw images to be analyzed thereby applying all corrections equally for all comparison groups. After background subtraction the greyscale image is converted into a binary image, and the sum of white pixels in each individual image is recorded.

Oxygen consumption

Oxygen consumption and mitochondrial parameters in intact cells were obtained using the XF24 Extracellular Flux Analyzer equipped with a FluxPak mini kit (#100867-100) from Seahorse Biosciences. In this system, oxygen consumption rates are calculated from 4 independent measurements obtained at 5 min intervals at baseline and after addition of specific drugs. For each experiment, the means from 3 replicate wells were recorded. For assessment of mitochondrial parameters, the values for the 4 independent measurements recorded for each condition were averaged, and parameters calculated as follows: ATP-linked respiration = basal OCR - oligomycin OCR; Proton leak = oligomycin OCR - rotenone+antimycin OCR; maximal capacity= FCCP OCR; reserve capacity = FCCP OCR – basal OCR; non-mitochondrial respiration = rotenone + antimycin OCR. Values presented are the means and s.e.m. of 4 independent experiments. For assessment of GDP sensitivity, cells were detached using trypsin/collagenase and suspended in respiration buffer[41], permeabilized with 20 μg/ml digitonin in respiration buffer for 5 minutes, washed again and oxygen consumption measured at 1 sec intervals using a Clark-type Oxygraph Plus recorder

(Hansatech Instruments). Oxygen consumption rates were expressed as the slopes of the linear regression fits for each trace, derived from a minimum of 300 points, after each addition. GDP was used at a final concentration of 1 mM.

Mice

All animal use was in accordance with the guidelines of the Animal Care and Use Committee of the University of Massachusetts Medical School. For all experiments reported male NOD.Cg-PrkdcscidIl2rgtm1Wjl/SzJ (NOD-scid IL2rγnull, NSG) mice[40] were used, at 12–14 weeks of age. Mice were obtained from the Jackson Laboratory. Mice were injected subcutaneously with Matrigel or cells suspended in Matrigel After the times indicated, animals were sacrificed and tissues were removed for further study. Where indicated mice were fed 60% HFD (Research Diets, Inc. D12492). Glucose tolerance curves were performed with 2g/Kg glucose after 8 or16h fasting, as indicated. The sample size chosen for glucose tolerance tests, temperature recordings and hyperinsulinemic-euglucemic clamp studies were based on preliminary data in control mice to determine variance for each parameter. Male animals of similar age bred under the same conditions were randomly assigned to Matrigel or cells, or to non-stimulated or forskolin-stimulated cells, and the investigator conducting the glucose tolerance tests, hyperinsulinemic-euglycemic clamps, and serum adiponectin measurements was blinded to the group (matrigel or cells, normal diet or HFD) allocation.

Affymetrix arrays

Total RNA was isolated using TRIzol. Affymetrix protocols were followed for the preparation of cRNA, which was hybridized to HTA-2.0 arrays. Raw expression data collected from an Affymetrix HP GeneArrayScanner was normalized across all data sets using the RMA algorithm as implemented by the Affymetrix Expression Console. Expression analysis was performed using the Affymetrix Transcriptome Analysis Console v. 3.0. The data discussed in this publication have been deposited in NCBI's Gene Expression Omnibus and are accessible through GEO Series accession number GSE73385.

Hyperinsulinemic-euglycemic clamp

Survival surgery was performed at 5~6 days before clamp experiments to establish an indwelling catheter in the jugular vein. On the day of the clamp experiment, mice were fasted overnight (~15 hrs), and a 2-hr hyperinsulinemic-euglycemic clamp was conducted in conscious mice with a primed and continuous infusion of human insulin (150 mU/kg body weight priming followed by 2.5 mU/kg/min; Humulin, Eli Lilly & Company, Indianapolis, IN, USA). To maintain euglycemia, 20% glucose was infused at variable rates during clamps. Whole body glucose turnover was assessed with a continuous infusion of [3-^{3}H]glucose (PerkinElmer, Waltham, MA, USA), and 2-7deoxy-D-[1-^{14}C]glucose (2-[^{14}C]DG) was administered as a bolus (10 μCi) at 75 min after the start of clamps to measure insulin-stimulated glucose uptake in individual organs.

Statistical analyses

RT-PCR results are presented as means of technical replicates with error range indicated. Experiments shown are representative, and have been repeated a minimal of 5 times with cells derived from different individuals undergoing panniculectomy surgery, with no *a priori* selection. The number of animal chosen for glucose tolerance tests, temperature recordings and hyperisnulinemic-euglucemic clamp studies were based on preliminary data in normal control mice to determine variance for each parameter. Software employed was GraphPad Prism v.6. To compare groups with normally distributed values, 2-tailed unpaired Student t-tests were used. When normality could not be determined, the Mann-Whitney test was used. Data are presented as mean values ± s.e.m., or range between technical replicates when experiments were representative, as indicated in each figure legend. *P*-values are indicated in each case. All representative experiments have been repeated a minimum of 5 times with tissue from different individuals, with similar results.

Supplementary Material

Refer to Web version on PubMed Central for supplementary material.

Acknowledgements

This study was funded by National Institutes of Health grants R01DK089101 (SC), R24OD018259 (MAB), R01DK089185 (MPC), R01-DK080756, R01-DK079999, R24-DK090963, and U24-DK093000 (J.K.K), and American Heart Association grant 12FTF11260010 (TPF). The authors acknowledge use of the UMASS Flow Cytometry Core, UMASS Genomics Core, UMASS Mouse Phenotyping Center, and UMASS Morphology Core in the conduct of these studies.

References

1. Collins S. A heart-adipose tissue connection in the regulation of energy metabolism. Nature reviews. Endocrinology. 2014; 10:157–163.
2. Lee YH, Petkova AP, Mottillo EP, Granneman JG. In vivo identification of bipotential adipocyte progenitors recruited by beta3-adrenoceptor activation and high-fat feeding. Cell metabolism. 2012; 15:480–491. [PubMed: 22482730]
3. Shabalina IG, et al. UCP1 in brite/beige adipose tissue mitochondria is functionally thermogenic. Cell reports. 2013; 5:1196–1203. [PubMed: 24290753]
4. Harms M, Seale P. Brown and beige fat: development, function and therapeutic potential. Nature medicine. 2013; 19:1252–1263.
5. Nedergaard J, Bengtsson T, Cannon B. Unexpected evidence for active brown adipose tissue in adult humans. American journal of physiology. Endocrinology and metabolism. 2007; 293:E444–E452. [PubMed: 17473055]
6. Cypess AM, et al. Identification and importance of brown adipose tissue in adult humans. The New England journal of medicine. 2009; 360:1509–1517. [PubMed: 19357406]
7. van Marken Lichtenbelt WD, et al. Cold-activated brown adipose tissue in healthy men. The New England journal of medicine. 2009; 360:1500–1508. [PubMed: 19357405]
8. Lidell ME, Betz MJ, Enerback S. Two types of brown adipose tissue in humans. Adipocyte. 2014; 3:63–66. [PubMed: 24575372]
9. Crandall DL, Hausman GJ, Kral JG. A review of the microcirculation of adipose tissue: anatomic, metabolic, and angiogenic perspectives. Microcirculation. 1997; 4:211–232. [PubMed: 9219215]
10. Han J, et al. The spatiotemporal development of adipose tissue. Development. 2011; 138:5027–5037. [PubMed: 22028034]

11. Bouloumie A, Lolmede K, Sengenes C, Galitzky J, Lafontan M. Angiogenesis in adipose tissue. Ann Endocrinol (Paris). 2002; 63:91–95. [PubMed: 11994668]
12. Tang W, et al. White fat progenitor cells reside in the adipose vasculature. Science. 2008; 322:583–586. [PubMed: 18801968]
13. Gupta RK, et al. Zfp423 expression identifies committed preadipocytes and localizes to adipose endothelial and perivascular cells. Cell metabolism. 2012; 15:230–239. [PubMed: 22326224]
14. Gealekman O, et al. Depot-specific differences and insufficient subcutaneous adipose tissue angiogenesis in human obesity. Circulation. 2011; 123:186–194. [PubMed: 21200001]
15. Tran KV, et al. The vascular endothelium of the adipose tissue gives rise to both white and brown fat cells. Cell metabolism. 2012; 15:222–229. [PubMed: 22326223]
16. van de Vyver M, Andrag E, Cockburn IL, Ferris WF. Thiazolidinedione-induced lipid droplet formation during osteogenic differentiation. The Journal of endocrinology. 2014; 223:119–132. [PubMed: 25210048]
17. Wu J, et al. Beige adipocytes are a distinct type of thermogenic fat cell in mouse and human. Cell. 2012; 150:366–376. [PubMed: 22796012]
18. Cypess AM, et al. Activation of human brown adipose tissue by a beta3-adrenergic receptor agonist. Cell metabolism. 2015; 21:33–38. [PubMed: 25565203]
19. Cousin B, et al. Occurrence of brown adipocytes in rat white adipose tissue: molecular and morphological characterization. Journal of cell science. 1992; 103(Pt 4):931–942. [PubMed: 1362571]
20. Orlicky DJ, Monks J, Stefanski AL, McManaman JL. Dynamics and molecular determinants of cytoplasmic lipid droplet clustering and dispersion. PloS one. 2013; 8:e66837. [PubMed: 23825572]
21. Marcinkiewicz A, Gauthier D, Garcia A, Brasaemle DL. The phosphorylation of serine 492 of perilipin a directs lipid droplet fragmentation and dispersion. The Journal of biological chemistry. 2006; 281:11901–11909. [PubMed: 16488886]
22. Zhang Y, Matheny M, Zolotukhin S, Tumer N, Scarpace PJ. Regulation of adiponectin and leptin gene expression in white and brown adipose tissues: influence of beta3-adrenergic agonists, retinoic acid, leptin and fasting. Biochimica et biophysica acta. 2002; 1584:115–122. [PubMed: 12385894]
23. Behan JW, et al. Activation of adipose tissue macrophages in obese mice does not require lymphocytes. Obesity. 2013; 21:1380–1388. [PubMed: 23754826]
24. Xiao C, Goldgof M, Gavrilova O, Reitman ML. Anti-obesity and metabolic efficacy of the beta3-adrenergic agonist, CL316243, in mice at thermoneutrality compared to 22 degrees C. Obesity. 2015; 23:1450–1459. [PubMed: 26053335]
25. Hocking SL, et al. Subcutaneous fat transplantation alleviates diet-induced glucose intolerance and inflammation in mice. Diabetologia. 2015; 58:1587–1600. [PubMed: 25899451]
26. Wang GX, et al. The brown fat-enriched secreted factor Nrg4 preserves metabolic homeostasis through attenuation of hepatic lipogenesis. Nature medicine. 2014; 20:1436–1443.
27. Jackson RS, et al. Obesity and impaired prohormone processing associated with mutations in the human prohormone convertase 1 gene. Nature genetics. 1997; 16:303–306. [PubMed: 9207799]
28. Benzinou M, et al. Common nonsynonymous variants in PCSK1 confer risk of obesity. Nature genetics. 2008; 40:943–945. [PubMed: 18604207]
29. Denning GM, et al. Proenkephalin expression and enkephalin release are widely observed in non-neuronal tissues. Peptides. 2008; 29:83–92. [PubMed: 18082911]
30. Miller AM, et al. Interleukin-33 induces protective effects in adipose tissue inflammation during obesity in mice. Circulation research. 2010; 107:650–658. [PubMed: 20634488]
31. Brestoff JR, et al. Group 2 innate lymphoid cells promote beiging of white adipose tissue and limit obesity. Nature. 2015; 519:242–246. [PubMed: 25533952]
32. Shinoda K, et al. Genetic and functional characterization of clonally derived adult human brown adipocytes. Nature medicine. 2015; 21:389–394.
33. Xue R, et al. Clonal analyses and gene profiling identify genetic biomarkers of the thermogenic potential of human brown and white preadipocytes. Nature medicine. 2015; 21:760–768.

34. Nishio M, et al. Production of functional classical brown adipocytes from human pluripotent stem cells using specific hemopoietin cocktail without gene transfer. Cell metabolism. 2012; 16:394–406. [PubMed: 22958922]

35. Elias I, et al. Adipose tissue overexpression of vascular endothelial growth factor protects against diet-induced obesity and insulin resistance. Diabetes. 2012; 61:1801–1813. [PubMed: 22522611]

36. Sun K, et al. Dichotomous effects of VEGF-A on adipose tissue dysfunction. Proceedings of the National Academy of Sciences of the United States of America. 2012; 109:5874–5879. [PubMed: 22451920]

37. Chang L, et al. Loss of perivascular adipose tissue on peroxisome proliferator-activated receptor-gamma deletion in smooth muscle cells impairs intravascular thermoregulation and enhances atherosclerosis. Circulation. 2012; 126:1067–1078. [PubMed: 22855570]

38. Fitzgibbons TP, et al. Similarity of mouse perivascular and brown adipose tissues and their resistance to diet-induced inflammation. American journal of physiology. Heart and circulatory physiology. 2011; 301:H1425–H1437. [PubMed: 21765057]

Online Methods References

39. Rojas-Rodriguez R, et al. Adipose tissue angiogenesis assay. Methods in enzymology. 2014; 537:75–91. [PubMed: 24480342]

40. Brehm MA, et al. Engraftment of human HSCs in nonirradiated newborn NOD-scid IL2rgamma null mice is enhanced by transgenic expression of membrane-bound human SCF. Blood. 2012; 119:2778–2788. [PubMed: 22246028]

41. Shabalina IG, Kramarova TV, Nedergaard J, Cannon B. Carboxyatractyloside effects on brown-fat mitochondria imply that the adenine nucleotide translocator isoforms ANT1 and ANT2 may be responsible for basal and fatty-acid-induced uncoupling respectively. The Biochemical journal. 2006; 399:405–414. [PubMed: 16831128]

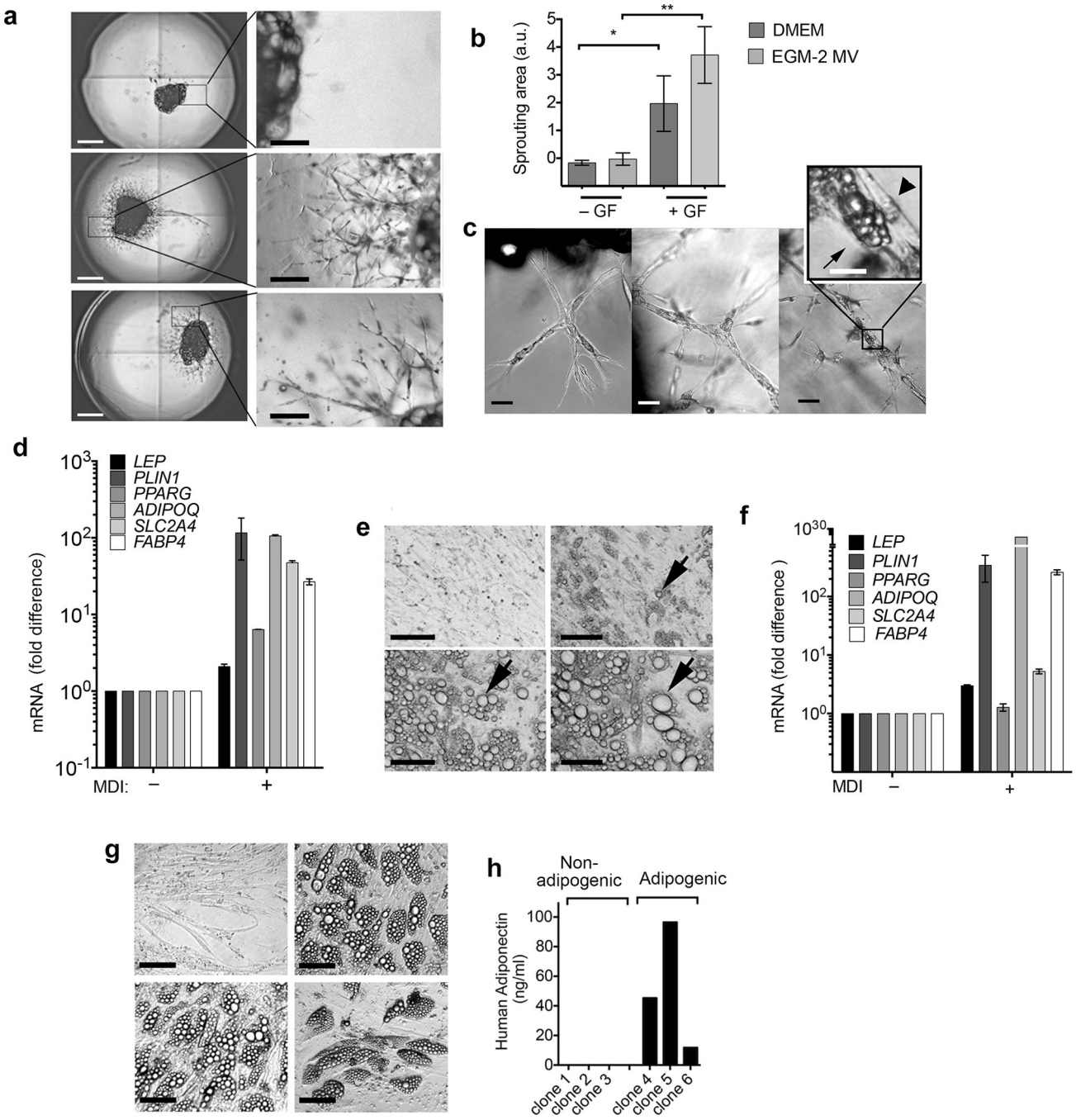

Figure 1.

Proliferation of human adipogenic precursors requires angiogenesis. All RT-PCR results are expressed as the fold over the minimum detectable value in the series, and represent the means and range of 2 technical replicates, of representative experiments that have been replicated a minimum of three times with cells from separate individuals. In cases where error bars are not apparent, replicates were too close to result in a visible range. **(a)** Explant growth in DMEM (top), DMEM + angiogenic growth factors (middle) or EGM-2 MV + angiogenic growth factors (bottom). Scale bars, 1 cm (left panels) and 200 μm (right panels).

(b) Growth area (arbitrary units) from explants grown for 11 days in the absence (− GF) or presence (+ GF) of angiogenic growth factors. Plotted are means and s.e.m, from 6 explants per condition from 2 different individuals ($n = 12$). Statistical significance was calculated using the Mann Whitney test $*P < 0.05$, $**P < 0.01$. **(c)** High resolution representative images of explants ($n = 27$ images per time point) grown for 5 (left), 12 (middle) or 18 (right) days, exposed to MDI at day 12. Arrowheads indicate elongated cells forming the sprouts, and arrows indicate lipid droplets. Scale bars, 200 μm and 50 μm (inset). (**d**) RT-PCR for genes indicated in non-differentiated (− MDI) or differentiated (+ MDI) explants 7 days after induction of differentiation. **(e)** A representative field ($n = 30$ images from independent wells) of capillary network cells at days 0 (top left), 6 (top right), 12 (bottom left) and 18 (bottom right) after induction of differentiation; arrows indicate growth of lipid droplets within a single adipocyte. Scale bars, 50 μm. **(f)** RT-PCR for genes indicated in non-differentiated (− MDI) or differentiated (+ MDI) cells seven days after induction of differentiation. **(g)** Example images ($n = 1$, though 35 independent clones were examined in total) of three adipogenic and one non-adipogenic clones identified by lipid droplet content, Scale bars, 50 μm. **(h)** Human adiponectin concentration detected in culture medium from three non-adipogenic and three adipogenic clones.

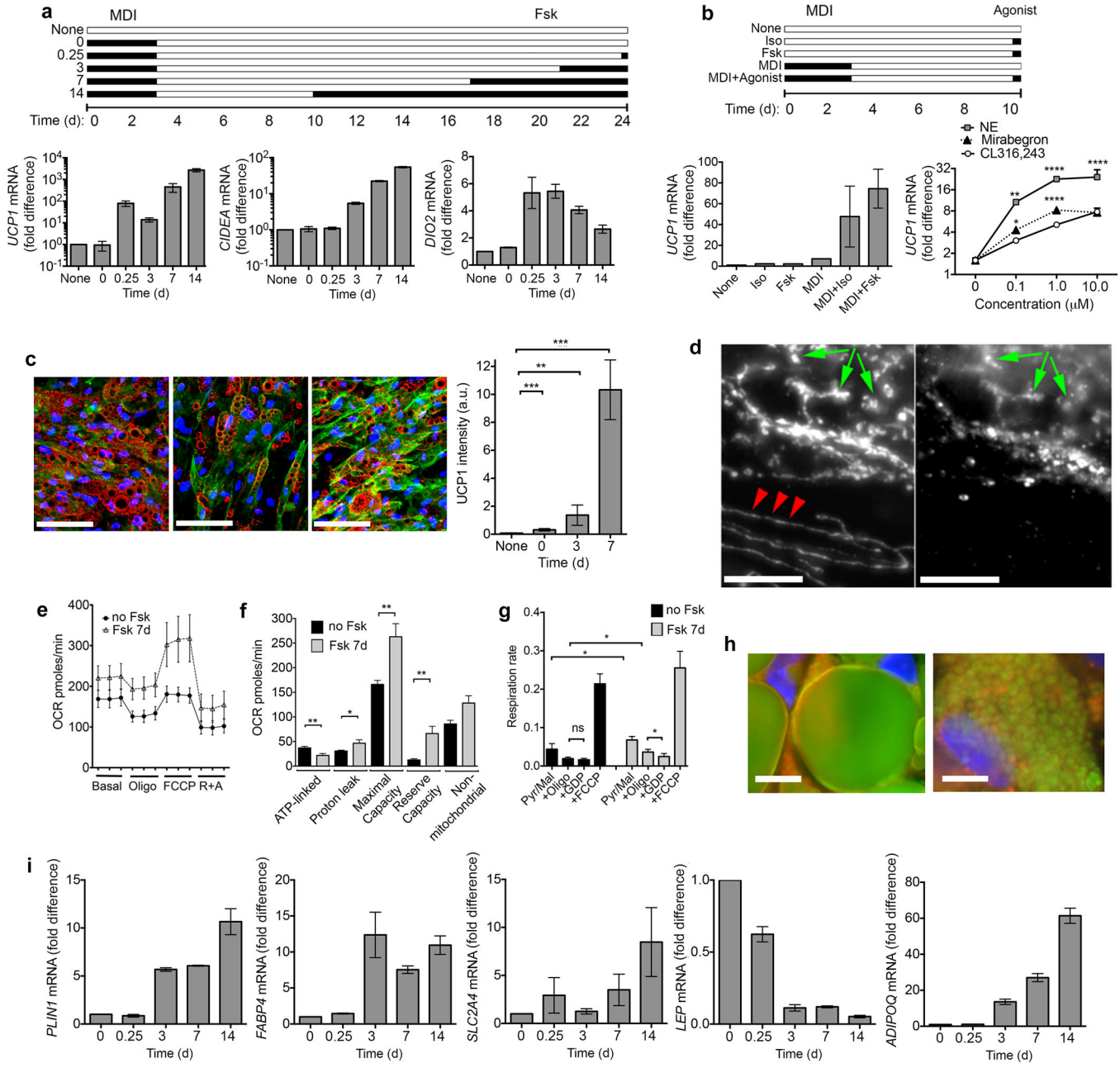

Figure 2.

Induction of human ‘brite/beige’ phenotype in adipocytes derived from capillary networks. **(a)** Experimental scheme (top) and RT-PCR of indicated genes (bottom), expressed as the fold over the minimum detectable value in the series. 0.25d refers to 6h. Shown are means and range of 2 technical replicates. In cases where error bars are not apparent, replicates were too close to result in a visible range. These results have been replicated with cells from 3 separate individuals. **(b)** Experimental scheme (top) and *UCP1* mRNA expression (bottom left) in cells exposed to isoproterenol (Iso) or forskolin (Fsk) as indicated in the scheme, or in response to different concentrations of adrenergic agonists (bottom right). Plotted are means and s.e.m. of 3 biological replicates ($n = 3$); statistical difference relative to

CL316,243 was determined at each concentration using Student t-tests corrected for multiple comparisons using the Holm-Sidak method *$P < 0.05$, **$P < 0.01$, ****$P < 0.0001$. **(c)** Representative images ($n = 30$ images (10 fields each of cells from 3 separate individuals)) of differentiated cells exposed to Fsk for 0 (left panel), 3 (middle panel) and 7 (right panel) days showing UCP1 (green), lipid droplets (red), and nuclei (blue). Scale bars, 200 μm. Plotted are means and s.e.m. of UCP1 staining intensity from 2 fields per coverslip, of cells from 3 different individuals ($n = 6$). Statistical significance was assessed using the Mann-Whitney test versus non-differentiated cells, **$P < 0.01$ ***$P < 0.001$. **(d)** Mitochondrial Hsp70 (left panel) and UCP1 (right panel) in adipocytes exposed to Fsk for 1 week. Arrowheads indicate linear mitochondrial structures in cell devoid of UCP1. Arrows indicate rounded mitochondrial structures containing both UCP1 and Hsp70. Scale bars, 20 μm. **(e)** Oxygen consumption by adipocytes exposed to vehicle or Fsk for 1 week. Plotted are the means and s.e.m. of 4 experiments assayed in triplicate ($n = 4$). **(f)** Summary data for oxygen consumption parameters, calculated as described in Online methods, derived from the means and s.e.m. of cells from 4 separate individuals assayed in triplicate ($n = 4$). Statistical significance was assessed using 2-tailed unpaired Student t-tests: *$P < 0.05$, **$P < 0.005$. **(g)** Oxygen consumption rate by digitonin-permeabilized adipocytes exposed to vehicle or Fsk for 1 week. Plotted are the means and s.e.m. of four experiments (n=4). Statistical significance assessed using 2-tailed unpaired Student t-tests *$P < 0.05$. ns, not significant. **(h)** Lipid droplets (green), mitochondria (red) and nuclei (blue) in adipocytes without (left) or with (right) exposure to Fsk for 14 days. Scale bars, 20 μm. **(i)** RT-PCR of indicated genes, expressed as the fold relative to t = 0. Shown are means and range of 2 technical replicates. These results have been replicated a minimum of 3 times with cells from separate individuals.

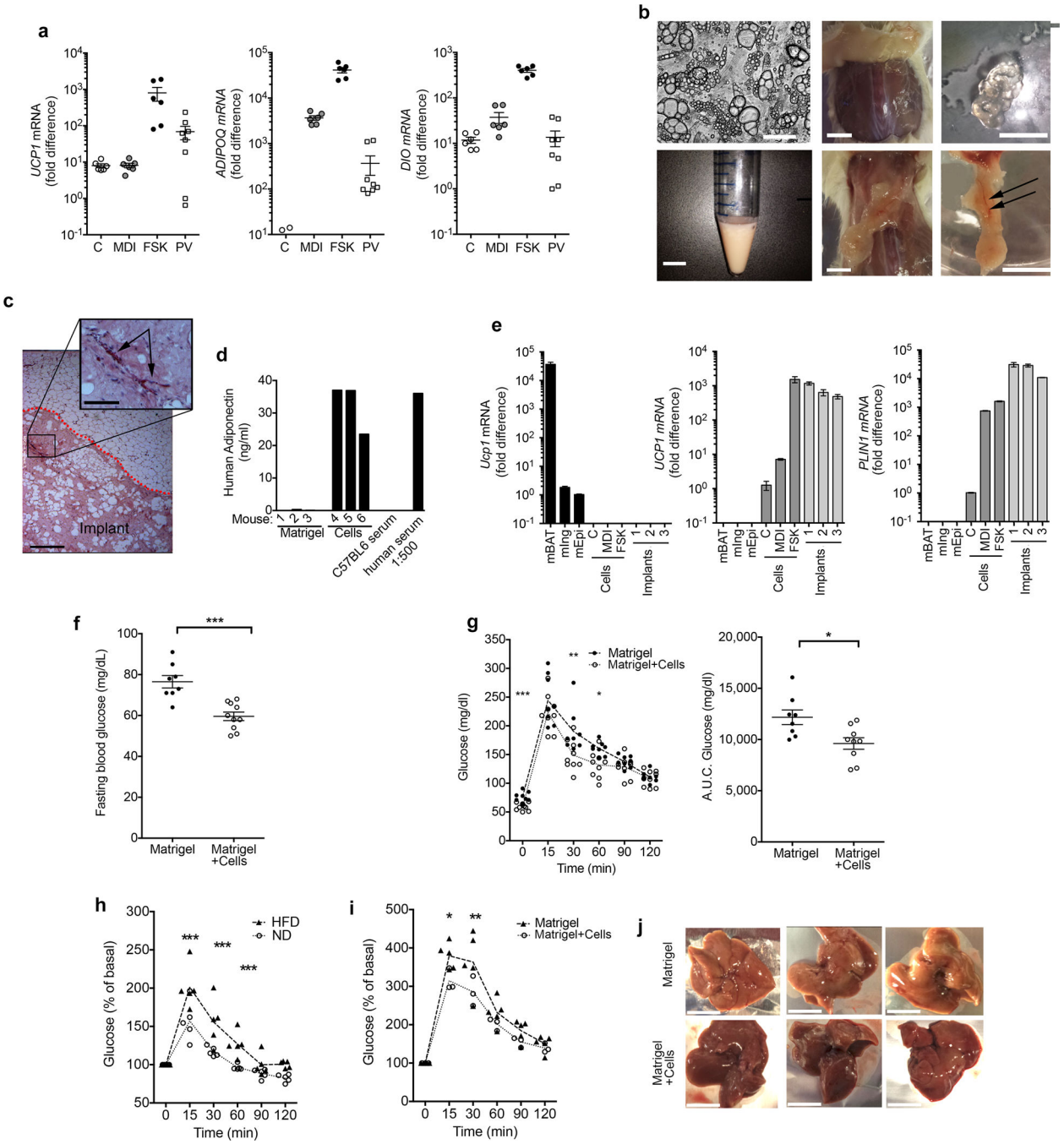

Figure 3.

Characteristics and metabolic effects of human ‘brite/beige’ adipocytes derived from capillary networks. **(a)** RT-PCR for indicated genes in non-differentiated (C), differentiated (MDI), and forskolin-treated adipocytes (FSK), and perivascular adipose tissue (PV). Values represent fold difference over the lowest detectable value in the series for the respective probe set. Plotted are means and s.e.m. from 2 technical replicates of samples from 3 (cells) or 4 (PV) individuals. **(b)** Phase image of cells for implantation (top left),; suspension of cells (bottom left); dorsal area of mouse injected with Matrigel alone (top middle); collected

remnants of the hydrogel (top right); dorsal area of mouse injected with cells (bottom middle); excised adipose structure (bottom right, scale bar) displaying vascularization (arrows). Scale bars, 100 μm (top left) and 1 cm. **(c)** Representative H&E staining of implant (n = 40 sections with 5 sections from each of 8 independent implants) ; dotted red line separating implant from surrounding mouse adipose tissue, blood vessels within the implant (arrow). Scale bars, 300 μm and 75 μm (inset). Similar results were seen in 8 additional implants. **(d)** Human adiponectin in sera from 6 mice implanted with either Matrigel alone or with cells in Matrigel, in serum from a control C57BL6 mouse, and in a 1:500 dilution of normal human serum. **(e)** RT-PCR for mouse *Ucp1*, human *UCP1* and human *PLIN1* in mouse adipose depots (mBAT, mIng and mEpi), human capillary-derived cells (C, MDI and FSK), and adipose structures from three mice, excised 7 weeks following implantation. Values represent the fold difference relative to the lowest detectable value in the series for each respective probe set, a value of 0 was given to non-detectable values. Error bars represent range of 2 technical replicates. **(f)** Fasting glucose levels, **(g)** Glucose tolerance curves (left) and areas under the curve (A.U.C) of the glucose excursion after 16h fast in male mice implanted with Matrigel (n = 8) or Matrigel+cells (n = 10). **(h)** Glucose tolerance curves after an 8 h fast in mice housed at 30°C for 2 weeks, fed a normal (n = 5) or a 60% HFD (n = 5). **(i)** Glucose tolerance curves after 11 weeks of 60% HFD feeding and an 8 h fast in mice housed at 30°C, implanted with either Matrigel (n = 5) or Matrigel+cells (n = 3) after 2 weeks of a HFD. Statistical analysis was performed using 2-tailed unpaired Student-t tests at each time point of glucose tolerance curves, and Mann-Whitney test between groups for fasting blood glucose and area under the curves. *P < 0.05, **P < 0.01, ***P < 0.0001. **(j)** Livers from mice used in **i** immediately following sacrifice at 11 weeks. Scale bars, 1 cm.

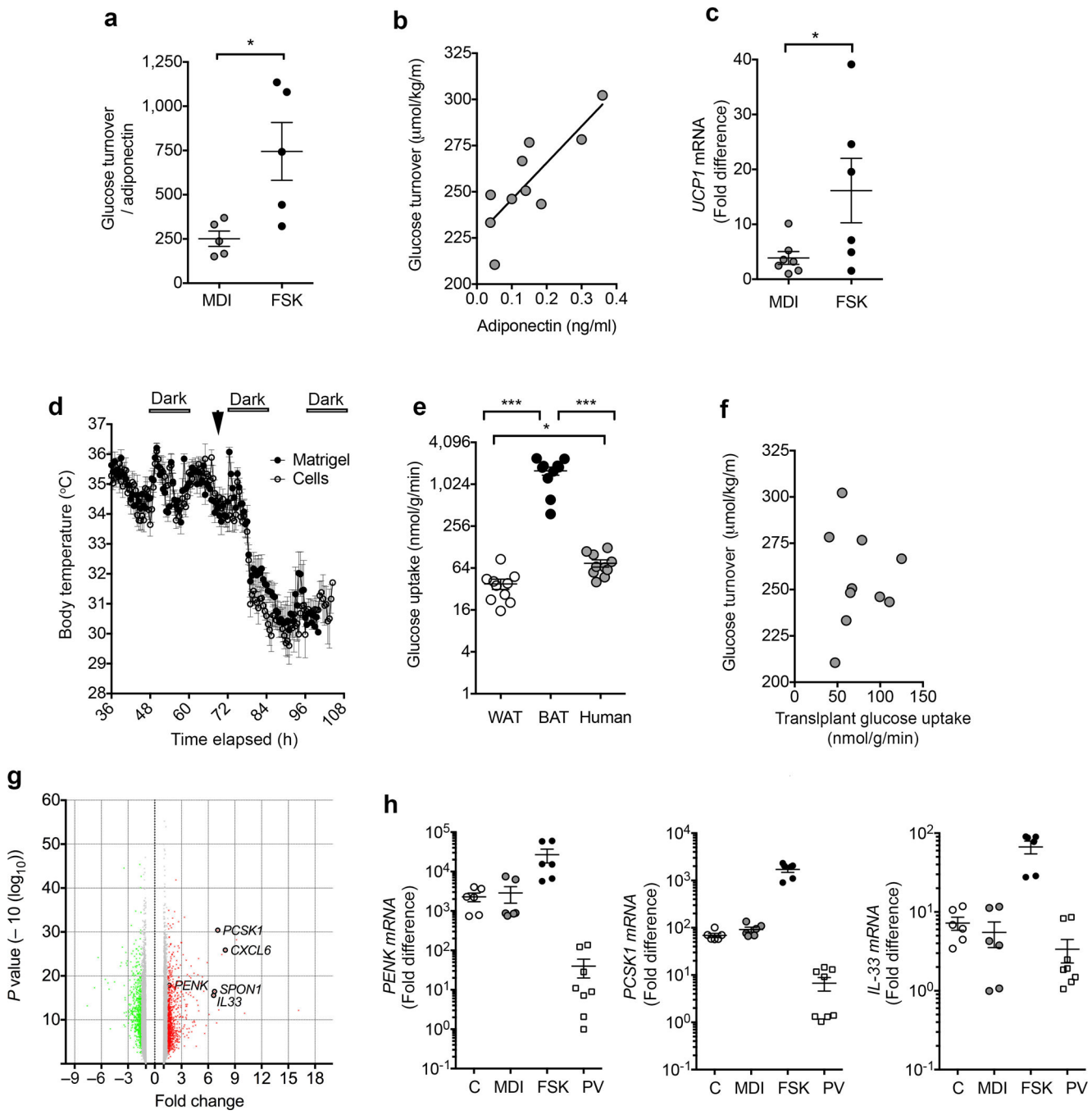

Figure 4.

Mechanism for metabolic effects of human 'brite/beige' adipocytes. **(a)** Glucose turnover (µmol/Kg/min) normalized to serum human adiponectin (ng/ml) in male mice implanted with non-stimulated (MDI, $n = 5$) or forskolin-stimulated (FSK, $n = 5$) adipocytes, seven weeks prior to hyperinsulinemic-euglycemic glucose clamps. Statistical analysis was performed using the Mann-Whitney test, $*P < 0.05$. **(b)** Relationship between serum human adiponectin levels and glucose turnover in implanted mice ($n = 10$). Linear regression P value = 0.0027, $R^2 = 0.601$. **(c)** RT-PCR for human *UCP1* in implanted cell structures from

mice studied in **a**. Statistical analysis was done using unpaired 2-tailed Student t-test, $*P < 0.05$. **(d)** Temperature recordings from subcutaneous iButtons in mice implanted with Matrigel or cells 7 weeks following implantation. Arrow represents time at which mice were placed at 5°C. **(e)** Glucose uptake into epididymal fat (WAT), interscapular brown fat (BAT) and implanted cell structures from mice studied in **b**, $n = 10$. Statistical analysis was performed using unpaired 2-tailed Student-t tests $*P < 0.05$, $***P < 0.0001$. **(f)** Relationship between glucose uptake into implanted cell structures and glucose turnover ($n = 10$). **(g)** Volcano plot of differential gene expression in adipocytes without or with forskolin treatment for 7 days, indicating genes of interest. **(h)** RT-PCR of *PCSK1, PENK* and *IL-33* expression in non-differentiated (C), differentiated (MDI), and forskolin-treated adipocytes (FSK), and perivascular adipose tissue (PV). Values represent fold difference over the lowest detectable value in the series for the respective probe set. Plotted are means and s.e.m. from 2 technical replicates of samples from 3 (cells) or 4 (PV) individuals.